LA-UR-19-24732 (Accepted Manuscript)

Compact readout of large CLYC scintillators with silicon photomultipler arrays

West, Stephen Thomas
Beckman, Darrel T.
Coupland, Daniel David Schechtman
Dallmann, Nicholas
Hardgrove, Craig James
Mesick, Katherine Elizabeth
Stonehill, Laura Catherine

To be published in: Nuclear Instruments and Methods in Physics Research Section A: Accelerators, Spectrometers, Detectors and Associated Equipment

DOI to publisher's version: 10.1016/j.nima.2019.162928

Permalink to record: http://permalink.lanl.gov/object/view?what=info:lanl-repo/lareport/LA-UR-19-24732

Journal Pre-proof

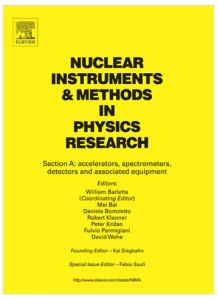

Compact readout of large CLYC scintillators with silicon photomultipler arrays

Stephen West, Darrel Beckman, Daniel Coupland, Nicholas Dallmann, Craig Hardgrove, Katherine Mesick, Laura Stonehill

PII: S0168-9002(19)31330-0
DOI: https://doi.org/10.1016/j.nima.2019.162928
Reference: NIMA 162928

To appear in: *Nuclear Inst. and Methods in Physics Research, A*

Received date : 12 June 2019
Revised date : 4 October 2019
Accepted date : 5 October 2019

Please cite this article as: S. West, D. Beckman, D. Coupland et al., Compact readout of large CLYC scintillators with silicon photomultipler arrays, *Nuclear Inst. and Methods in Physics Research, A* (2019), doi: https://doi.org/10.1016/j.nima.2019.162928.

Compact Readout of Large CLYC Scintillators with Silicon Photomultipler Arrays

Stephen West[a,b,*], Darrel Beckman[a], Daniel Coupland[a], Nicholas Dallmann[a], Craig Hardgrove[b], Katherine Mesick[a], Laura Stonehill[a]

[a] *Los Alamos National Laboratory, Los Alamos, NM 87545, USA*
[b] *Arizona State University, Tempe, AZ 85287, USA*

Abstract

Compact readout of a large (5 x 5 x 5 cm^3) CLYC scintillator was demonstrated with a 8 x 8 array of 6mm silicon photomultipliers (SiPMs, specifically, a SensL ArrayJ-60035-64P) and an optimized amplification and summing circuit. Read out by the SiPM array, the crystal yielded an energy resolution of 5.5% at 662 keV and a figure of merit of 3.5, equivalent to the performance achieved with a 3-inch Hamamatsu R6233-100 PMT. To reduce channel count and avoid individual amplification of each SiPM in the array, the standard outputs of 16 SiPMs were passively summed then amplified. A current feedback amplifier was used for each channel to provide the required fast response time. The four amplified channels were then passively summed resulting in a single signal channel. A custom laboratory setup, based on the PSD8C ASIC, was used to capture the output and provide time-gated integration for PSD computation. The compact volume, low bias voltage, and reduced mass of the SiPM array readout are desirable for space and national security applications.

Keywords: CLYC, silicon photomultipliers, readout electronics

1. Introduction

CLYC (Cs_2LiYCl_6) is an inorganic scintillator in the elpasolite family that is sensitive to both neutrons (primarily through the $^6Li(n,\alpha)t$ reaction) and gamma-rays. Gamma-ray and neutron interactions can be differentiated by their characteristic pulse shapes. Gamma-rays produce a scintillation light pulse marked by a faster rise and decay time as compared to neutron interaction waveforms [1].

CLYC is under study for a variety of applications where low size, weight, and power (SWaP) is desired. Because of CLYC's neutron and gamma-ray sensitivity, a single instrument is capable of detecting what would traditionally require two separate detectors. Los Alamos National Laboratory has developed handheld CLYC instruments for use in nuclear security applications [2, 3] as well as space-borne CLYC experimental instruments to assess the technology

*Corresponding author
Email address: stwest@asu.edu (Stephen West)

for next-generation national security missions [4]. CLYC is also being examined for use in gamma-ray and neutron detectors for planetary science applications.

To quantitatively distinguish neutron and gamma-ray interactions, we integrate the scintillation light pulse with different time gates. We define a pulse shape discrimination (PSD) parameter as the ratio of the delayed portion of the scintillation light pulse to the sum of the prompt and delayed segments:

$$PSD = \frac{A_{delayed}}{(A_{prompt} + A_{delayed})}. \quad (1)$$

Typical prompt (P) and delayed (D) integration windows are superimposed on the average waveforms shown in Figure 3.

The quality of neutron/gamma-ray discrimination in a particular energy range can be quantified using a figure of merit (FOM) parameter. In this paper, we standardize to an energy range 1 MeV wide centered on the neutron peak. We generate a histogram of PSD values within this energy range, which takes the form of two approximately normal distributions due to the different PSD of neutrons and gammas. We fit the neutron and gamma-ray distributions with Gaussians to identify the peak centroid (x) and the full width at half max ($FWHM$) of each. The FOM is then computed by dividing the difference between the centroids by the sum of their $FWHM$:

$$FOM = \frac{x_n - x_\gamma}{FWHM_n + FWHM_\gamma}. \quad (2)$$

Photomultiplier tubes (PMTs) have traditionally been used to read out CLYC detector volumes and are capable of realizing energy resolution as high as 3.9% at the 662 keV ^{137}Cs peak [5] and a FOM as high as 4.55 [6]. From a SWaP perspective, PMTs occupy a large volume, require kV-scale bias, and are delicate components requiring structural accommodations that lead to increased mass. While both science objectives and engineering constraints ultimately inform scintillator read-out design, maximizing the fraction of overall instrument mass and volume occupied by sensitive material yields benefits for any application. Silicon photomultipliers (SiPMs) are a solid state alternative to PMTs for detecting faint scintillation light. Individual SiPMs are arrays of thousands of avalanche photodiode pixels operating in a Geiger mode [7]. While individual SiPMs are quite small (e.g. SensL J-series are available in 3 mm x 3 mm, 4 mm x 4 mm, and 6 mm x 6 mm square formats), arrays of matched SiPMs with uniform output allow larger areas to be covered.

Previous testing at LANL of small CLYC volumes read out by single SiPMs achieved an energy resolution of 6.6% at 662 keV and a FOM of 2.2 (at room temperature) [8]. These experiments also revealed that the resolution of SiPM read-out CLYC to be insensitive to temperature with the neutron/gamma-ray discrimination improving at lower temperatures. In order to read out larger CLYC volumes, arrays of multiple SiPMs are required. Satisfactory energy resolution and pulse shape discrimination have been demonstrated with arrays of SiPMs on fast scintillators; however, these experiments required amplifying

the output of each individual SiPM prior to summing [9, 10]. For large arrays in a SWaP-constrained environment, the power consumption of individual SiPM amplification is undesirable.

Passively summing an array of SiPMs reduces the power and channel count requirements but also increases the effective capacitance. As multiple individual SiPMs are connected in parallel, their junction capacitance is summed. This increased capacitance (as compared to a single SiPM) reduces the output bandwidth, distorting the pulse shapes and diminishing the PSD capability. PSD is possible with an array of a few SiPMs but rapidly becomes impossible for larger arrays unless a more sophisticated approach is adopted.

We developed a summing, amplification, and digitization setup for large (64-element) arrays of SiPMs on large CLYC volumes. We describe the design of this readout board and present experimental results from a benchtop prototype.

2. Design of SiPM readout board

2.1. Design considerations

In order to use SiPMs as a drop-in replacement for PMTs in dual-mode, neutron and gamma-ray detection, the readout circuit must preserve both energy resolution and PSD. These two design goals impose different requirements on the readout circuitry. Achieving high energy resolutions requires that the full amplitude of the pulse be captured. Robust PSD (as indicated by higher FOM values) requires that the circuit responds quickly enough to capture the fast-acting scintillation mechanisms that distinguish gamma-ray from neutron interactions.

Gamma-ray spectroscopy requires that energy resolution be high enough to distinguish spectral lines of interest. For CLYC, the best energy resolutions are reported for smaller crystals (1 inch diameter) with larger crystals generally exhibiting broader resolution. For this work, we will measure and compare energy resolution at the ^{137}Cs 662 keV line, the 2614 keV ^{208}Tl line from the decay of ^{228}Th. We also report the energy resolution of the thermal neutron capture peak, although this is only moderately useful in quantifying performance. While the neutron capture process is monoenergetic with a 4783 keV Q-value, the scintillation efficiency of the resulting alpha and triton is lower than that of an electron, as is common in scintillators [11, 12], and depends on both temperature [13] and to some extent the specific crystal. Near room temperature, the resulting light output is similar to that of a 3.2 MeV gamma or electron (a.k.a. 3.2 MeV electron equivalent or 3.2 MeVee)[14], but the peak is broader than a mono-energetic gamma-ray line of that energy.

Multiple mechanisms produce scintillation light in a CLYC crystal with the relative contribution from each dependent on the type of interaction[5]. Achieving robust PSD requires a readout with sufficiently fast response to distinguish the faster pulse of a gamma-ray interaction from the slower pulse of a thermal neutron capture [1, 15]. For context, [1] reports a rise time of 16 ns for gamma-ray interactions versus 47 ns for a thermal neutron. The required PSD

FOM depends on the application, but a FOM of 1 is often considered a bare minimum. With an optimally placed cut, a FOM of 1 means that 0.9% of each distribution is counted as part of the other. At FOM=1.5, that number drops to 2×10^{-4}. However, those numbers assume perfectly Gaussian distributions of the PSD parameter, while reality often produces non-Gaussian tails to the distributions due to pulse pileup or odd triggering conditions, so preserving the exceptional PSD of CLYC is preferred.

2.2. SiPM readout

We developed a readout board for the 64 element SensL ArrayJ-60035-64P. The board provides a common bias, buffered through a 10 μF and 22 μF capacitance to ground, to all 64 SiPMs. The 64 elements in the array are divided into 4 quadrants each comprised of 16 SiPMs for summing and amplification. The bias supply for each quadrant has an additional 10 nF capacitance to ground for decoupling. Within a single quadrant, the standard output of each SiPM is passed through a 10 Ω series resistance before being passively summed at the common input to a LMH6703 current feedback operational amplifier. The amplifier is configured with a 390 Ω resistance in the feedback circuit, a 25 Ω resistance to ground on the non-inverting input, and a 50 Ω resistance in series with the output to a 50 Ω impedance RG-58 coaxial cable. The LMH6703 was biased with $\pm$5V and had 1 μF capacitance on each of the rails. In this configuration, each operational amplifier consumes approximately 60 mW with a bandwidth on the order of 500 MHz. The series resistance of 10 Ω was chosen to minimize the RC time constant between the SiPMs and amplifier without causing instability in the amplifier performance. Figure 1 shows the configuration of the common bias supply and a single quadrant of the summing and amplification circuit.

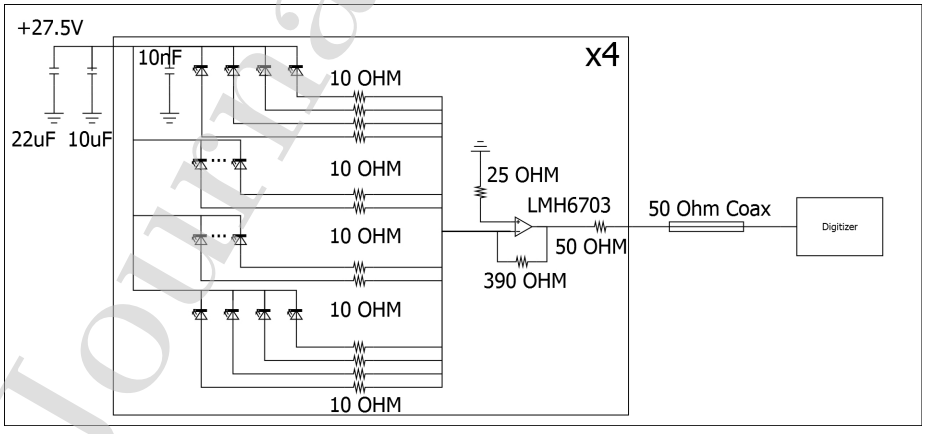

Figure 1: The readout circuit passively sums the standard outputs of 16 individaul SiPMs and amplifies the summed signal through a LMH6703 current feedback amplifier. The amplifier's $\pm$5V bias and 1 μF capacitance (on eachthe rails) are not shown.

3. Experimental setup

A 5 cm cube of CLYC was commercially procured from Radiation Monitoring Devices (RMD). The hygroscopic CLYC was packaged by RMD in a hermetically sealed aluminum enclosure (0.125" thick) with a quartz optical window (0.125" thick). This large volume CLYC detector was coupled to both a 3-inch Hamamatsu R6233-100 PMT and the SensL 64-SiPM array, using silicone-based optical grease and black electrical tape, in order to compare performance. Figure 2 shows both photodetectors placed atop the CLYC volume, prior to being wrapped with black electrical tape and enclosed in a dark box for measurements.

Figure 2: The SensL ArrayJ-60035-64P occupies substantially less volume than an equivalently sized Hamamatsu R6233-100 PMT. Both photodetetors are shown atop the 5 cm CLYC volume, prior to thoroughly wrapping the interface in black electrical tape, for scale.

3.1. PMT baseline

The CLYC volume was optically coupled to a 3-inch R6233-100 PMT to collect data for benchmarking the SiPM array performance. Figure 3 shows average waveforms recorded with an R6233-100 PMT. As expected, the gamma-ray

waveform exhibits a faster rise time due to the fast scintillation light components excited by the gamma-ray interaction. The FOM within a ±0.5 MeV window around the neutron peak was 3.5. The energy resolution achieved with this CLYC detector read out by the PMT was 5.5% FWHM at 662 keV. This was measured using an Amptek MCA-8000D multichannel analyzer after shaping the signal with a 6 μs shaping time.

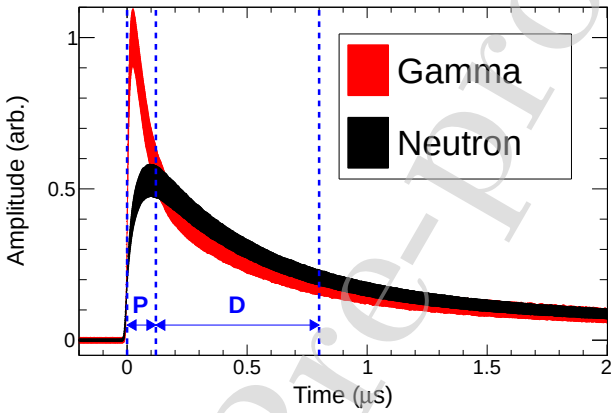

Figure 3: Average gamma and neutron waveforms recorded with a R6233 PMT. Standard prompt (P) and delayed (D) pulse shape integration windows are also indicated.

3.2. SiPM waveform digitization

Individual event waveforms were collected using an Agilent Acqiris DC282 10 bit, 2 Gsample/s waveform digitizer. The outputs of each of the 4 amplified channels (16 SiPMs/channel) were connected to form a single output. This single channel was connected to the Acqiris waveform digitizer. The digitizer's input voltage and offset were configured to appropriately scale the incoming signal without saturating. Waveforms were collected for interactions from a variety of neutron and gamma-ray sources. Examination of average waveforms informed the optimization of the readout circuit to provide suitable PSD.

3.3. SiPM time-gated integration

Data were also collected using a custom analog time-gated charge integration data acquisition system. The LANL-developed Custom Laboratory PSD System (CLPS) is capable of reading out eight channels with three time-gated integration windows. CLPS is based on the PSD8C application specific integrated circuit (ASIC) [16] that has also been used in LANL-developed handheld instruments [2, 3]. The detector was configured in the same fashion as for waveform digitization: all four amplified channels passively summed, then connected to the input of the CLPS system.

4. Results

4.1. Waveforms

Waveforms were acquired as a diagnostic to determine if the SiPM array's response time was sufficient for resolving the difference between neutron and gamma-ray interactions. Figure 4 shows example average waveforms acquired with the SiPM array and Acqiris high speed waveform digitizer. The difference in pulse height and shape between the gamma-ray and neutron average waveform has been preserved.

4.2. Time-gated integration results

Integral data was recorded using CLPS. The three gated integration windows were configured to cover the prompt (0-148 ns), delayed (176-476 ns), and total (0-10 μs) portions of the pulse. The prompt and delayed windows were determined by optimizing integration windows for the digitized waveforms to maximize FOM.

Figure 5 shows an energy spectra of ^{137}Cs. The energy resolution at the 662 keV peak was 5.5% FWHM. Energy resolution at moderate gamma-ray energies and the neutron capture peak was measured from a ^{252}Cf and ^{228}Th source. The 2.61 MeV ^{228}Th peak had a resolution of 2.7% FWHM. The 3.2 MeV ^{6}Li(n,α)t peak had a resolution of 3.8%.

PSD performance of the CLYC detector and SiPM array was examined by computing PSD values for events recorded from a ^{252}Cf and ^{228}Th source. Figure 6 shows a 2D histogram of PSD value versus energy. The resulting FOM was 3.5, indicating excellent neutron/gamma-ray discrimination.

4.3. Linearity analysis with high energy gamma-rays

The response linearity of the combined large CLYC volume and readout circuit was investigated by capturing data across a broad range of incident gamma-ray energies. Multiple runs were conducted with different sources, referenced to a ^{137}Cs line included in each data set. High energy gamma-rays were produced from an AmBe source as well as ^{56}Fe(n,g) interactions in an iron plate irradiated by a ^{252}Cf source. These setups produced 4.4 MeV and 7.6 MeV gamma-rays, respectively, along with single- and double-escape peaks. Acquiring the highest energy ^{56}Fe(n,g) gamma-rays required a lengthy integration time (overnight). To account for slow gain changes due to temperature fluctuations, the ^{56}Fe(n,g) data was matched every thirty minutes to the 2223 keV H(n,g) line. The H(n,g) line was in turn matched across other datasets taken with lower energy sources. A linear calibration was fit to the low energy gamma-ray peaks up to 2614 keV. Figure 7 shows this trendline, the low-energy reference peaks, and the high energy peaks from AmBe and ^{56}Fe(n,g). The high energy peaks match the low-energy derived trendline to within systematic uncertainties.

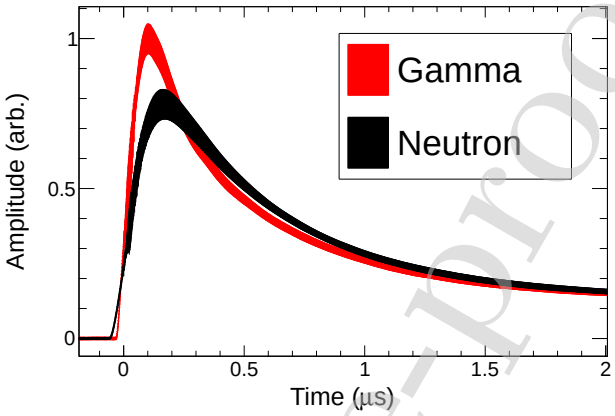

Figure 4: Average waveforms captured using the 64-SiPM array and high speed digitizer. The standard deviation between waveforms is shown by the filled region. The gamma-ray waveform is normalized to unity and the neutron waveform is normalized to have the same integral as the gamma-ray waveform.

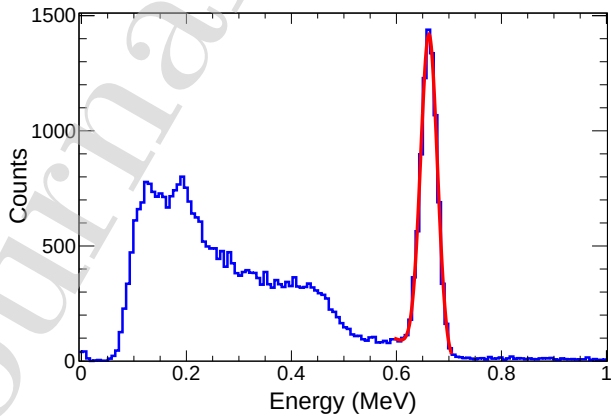

Figure 5: The 662 keV ^{137}Cs peak had a resolution of 5.5% FWHM. The Gaussian fit to the peak is shown in red.

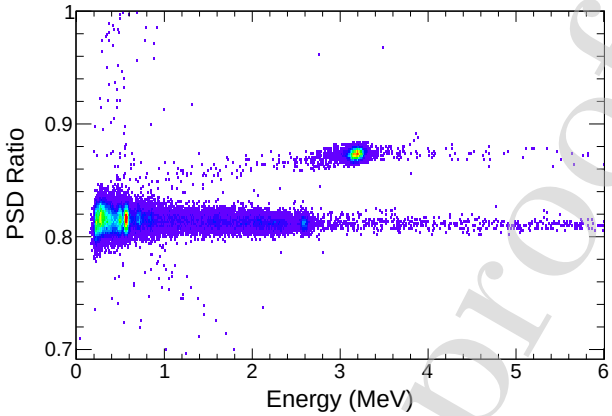

Figure 6: A 2D histogram of PSD versus energy indicates excellent neutron/gamma-ray discrimination with a FOM of 3.5.

5. Discussion and potential applications

5.1. Replacement for PMT

These results demonstrate that SiPM arrays can be used as a drop-in replacement for PMTs to perform dual-mode neutron/gamma-ray detection with large CLYC volumes (up to 5 x 5 x 5 cm^3). SiPMs have advantages over PMTs in that they do not require high voltage bias and are less susceptible to interference from magnetic fields. As opposed to the kV-scale bias required by PMTs, the SiPM array used for these experiments operated at a 27.5V bias. Removing high voltage power supplies simplifies instrument design and packaging. Magnetic fields can change the response of a PMT by affecting the trajectory of electrons between dynode stages; this is an appreciable effect even when changing the orientation of a PMT in the Earth's magnetic field [11]. As a solid state device, SiPMs are immune to these effects.

SiPMs also require less volume (as compared to PMTs) in an instrument design – critical for spaceflight and other applications where size is constrained. Table 1 shows the approximate volume envelope for the SensL 64-pixel array compared to alternative configurations with four Hamamatsu R11265 or one Hamamatsu R6233-100. Values represent the envelope occupied by the photodetector only as required readout electronics vary by application.

SiPMs are known to exhibit variation of breakdown voltage (and therefore gain) with temperature. SensL quotes a low value breakdown voltage temperature dependence of <21.5 mV/°C. Given that CLYC also has temperature-dependent effects [15], SiPM gain variation can be accounted for in post-processing as long as the temperature of the array is monitored during data acquisition.

5.2. Compact planetary science instrumentation

Two CLYC-based planetary science instruments are currently under development by the authors. The Elpasolite Planetary Ice and Composition Spectrom-

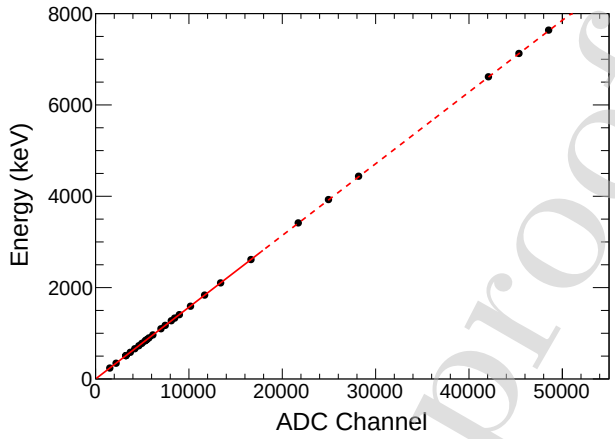

Figure 7: High energy AmBe and ^{56}Fe(n,g) gamma-ray lines match the linear trend observed at energies <2614 keV to within systematic uncertainties.

Table 1: Comparison of SiPM volume envelope with equivalent PMT readout configurations illustrate volume savings possible with a SiPM array.

Readout	Volume (cm^3)	SiPM Volume Reduction (%)
SensL 64 pixel SiPM array	26	-
Hamamatsu R11265 (x4)	80	67
Hamamatsu R6233-100	213	88

eter (EPICS) is a LANL instrument concept that maximizes the percentage of instrument volume devoted to detector material by using CLYC read out with SiPM arrays [17, 18, 19]. As a dual-mode detector, CLYC achieves in a single instrument what would typically require separate detectors (e.g. ^{3}He for neutrons and high purity germaium for gamma-rays). SiPM arrays are substantially lower-volume than PMTs and also permit packaging without concern for accommodating PMTs adjacent to the detector volumes.

Arizona State University (ASU) is developing the Miniature Neutron Spectrometer (Mini-NS), a compact CLYC-based neutron detector for the Lunar Polar Hydrogen Mapper (LunaH-Map) mission. LunaH-Map is a 6U CubeSat that will map hydrogen enrichments in cold traps at the Moon's south pole[20, 21]. The Mini-NS is designed to fit within an approximately 20x10x10 cm^3 (∼2U) envelope and uses eight Hamamatsu R11265 PMTs to read out eight 4x6.3x2 cm^3 CLYC volumes. Future versions of this CubeSat-class neutron detector could be made more compact, for an equivalent CLYC volume, by replacing PMTs with SiPM arrays. Additionally, a SiPM-based detector design would eliminate the high voltage power supplies in the current, PMT-based Mini-NS design.

Both the EPICS and Mini-NS instrument design could be adapted for landed

missions where they must operate within the dust environment of a planetary surface. Under these conditions, high voltage power supplies are susceptible to arcing. By requiring lower bias, SiPMs eliminate this risk and may enable longer-lived surface instruments.

6. Conclusion

We have developed and optimized a readout circuit for a 64 pixel SiPM array that preserves good energy resolution and pulse-shape discrmination in large CLYC volumes, thereby demonstrating that SiPMs can be used as a drop-in replacement for PMTs with CLYC dual-mode neutron/gamma-ray detectors. A 64 pixel SensL ArrayJ-60035-64P SiPM array, read out as a single channel, yields 5.5% FWHM energy resolution at 662 keV and a FOM of 3.5. This matches the performance of a R6233 PMT with the same crystal. The custom readout circuit uses a current feedback amplifier to achieve a sufficiently fast response time. The SiPM array and read-out circuit do not require high voltage power supply and can be accommodated in significantly less volume than an equivalent PMT and readout circuitry.

7. Acknowledgements

This work was supported by the Laboratory Directed Research and Development program of Los Alamos National Laboratory under project number 20170438ER.

The authors thank two anonymous reviewers for their constructive comments.

8. References

[1] N. D'Olympia, P. Chowdhury, C. J. Lister, J. Glodo, R. Hawrami, K. Shah, U. Shirwadkar, Pulse-shape analysis of CLYC for thermal neutrons, fast neutrons, and gamma-rays, Nuclear Instruments and Methods in Physics Research, Section A: Accelerators, Spectrometers, Detectors and Associated Equipment 714 (2013) 121–127. doi:10.1016/j.nima.2013.02.043.

[2] B. S. Budden, L. C. Stonehill, A. Warniment, J. Michel, S. Storms, N. Dallmann, D. D. Coupland, P. Stein, S. Weller, L. Borges, M. Proicou, G. Duran, J. Kamto, Handheld readout electronics to fully exploit the particle discrimination capabilities of elpasolite scintillators, Nuclear Instruments and Methods in Physics Research, Section A: Accelerators, Spectrometers, Detectors and Associated Equipment 795 (2015) 213–218. doi:10.1016/j.nima.2015.06.004.
URL http://dx.doi.org/10.1016/j.nima.2015.06.004

[3] B. S. Budden, L. C. Stonehill, N. Dallmann, M. J. Baginski, D. J. Best, M. B. Smith, S. A. Graham, C. Dathy, J. M. Frank, M. McClish, A Cs2LiYCl6:Ce-based advanced radiation monitoring device, Nuclear Instruments and Methods in Physics Research, Section A: Accelerators, Spectrometers, Detectors and Associated Equipment 784 (2015) 97–104. doi:10.1016/j.nima.2014.11.051.
URL http://dx.doi.org/10.1016/j.nima.2014.11.051

[4] D. D. Coupland, L. C. Stonehill, K. E. Mesick, J. P. Dunn, The SENSER CLYC Experiment, in: IEEE Nuclear Science Symposium and Medical Imaging Conference, 2016.

[5] J. Glodo, E. V. Loef, R. Hawrami, W. M. Higgins, A. Churilov, U. Shirwadkar, K. S. Shah, Selected Properties of Cs2LiYCl6, Cs2LiLaCl6, and Cs2LiLaBr6 Scintillators, IEEE Transactions on Nuclear Science 58 (1) (2011) 333–338.

[6] D. W. Lee, L. C. Stonehill, A. Klimenko, J. R. Terry, S. R. Tornga, Pulse-shape analysis of Cs2LiYCl6:Ce scintillator for neutron and gamma-ray discrimination, Nuclear Instruments and Methods in Physics Research, Section A: Accelerators, Spectrometers, Detectors and Associated Equipment 664 (1) (2012) 1–5. doi:10.1016/j.nima.2011.10.013.
URL http://dx.doi.org/10.1016/j.nima.2011.10.013

[7] SensL, An introduction to the silicon photomultiplier (2011) 1–16.
URL https://www.sensl.com/downloads/ds/TN - Intro to SPM Tech.pdf

[8] K. E. Mesick, L. C. Stonehill, J. T. Morrell, D. D. Coupland, Performance of several solid state photomultipliers with CLYC scintillator, 2015 IEEE Nuclear Science Symposium and Medical Imaging Conference, NSS/MIC 2015 (2015) 1–4arXiv:1512.01155, doi:10.1109/NSSMIC.2015.7581936.

[9] C. Betancourt, A. Blondel, R. Brundler, A. Dätwyler, Y. Favre, D. Gascon, S. Gomez, A. Korzenev, P. Mermod, E. Noah, N. Serra, D. Sgalaberna, B. Storaci, Application of large area SiPMs for the readout of a plastic scintillator based timing detector, Journal of Instrumentation 12 (11). doi:10.1088/1748-0221/12/11/P11023.

[10] G. A. de Nolfo, P. Bloser, J. DuMonthier, A. Garcia-Burgos, J. M. Ryan, G. Suarez, A neutron spectrometer for small satellite opportunities, 2015 IEEE Nuclear Science Symposium and Medical Imaging Conference (NSS/MIC) 6 (1) (2015) 1–3. doi:10.1109/NSSMIC.2015.7581897.
URL http://ieeexplore.ieee.org/document/7581897/

[11] G. F. Knoll, Radiation Detection and Measurement, Fourth Edition, John Wiley & Sons, Inc., 2010.

[12] J. Birks, The theory and practice of scintillation counting, Pergamon Press, Oxford, 1967.

[13] P. Menge, D. Richaud, Behavior of Cs2LiYCl6:Ce scintillator up to 175C, in: 2011 IEEE Nuclear Science Symposium Conference Record, 2011, pp. 1589–1601.

[14] A. Bessiere, P. Dorenbos, C. van Eijk, K. Krämer, H. Güdel, New Thermal Neutron Scintillators: Cs2LiYCl6:Ce3+ and Cs2LiYBr6:Ce3+, IEEE Transactions on Nuclear Science 51 (2004) 2970–2972.

[15] B. S. Budden, L. C. Stonehill, J. R. Terry, A. V. Klimenko, J. O. Perry, Characterization and investigation of the thermal dependence of Cs2LiYCl6: Ce3+(CLYC) waveforms, IEEE Transactions on Nuclear Science 60 (2) (2013) 946–951. doi:10.1109/TNS.2012.2215884.

[16] G. L. Engel, M. J. Hall, J. M. Proctor, J. M. Elson, L. G. Sobotka, R. Shane, R. J. Charity, Design and performance of a multi-channel, multi-sampling, PSD-enabling integrated circuit, Nuclear Instruments and Methods in Physics Research, Section A: Accelerators, Spectrometers, Detectors and Associated Equipment 612 (1) (2009) 161–170. doi:10.1016/j.nima.2009.10.058.
URL http://dx.doi.org/10.1016/j.nima.2009.10.058

[17] K. E. Mesick, L. C. Stonehill, D. D. S. Coupland, D. T. Beckman, S. T. West, S. F. Nowicki, N. A. Dallmann, S. A. Storms, W. C. Feldman, Elpasolite Planetary Ice and Composition Spectrometer (EPICS): A Low-Resource Combined Gamma-Ray and Neutron Spectrometer for Planetary Science, in: Submitted, 2019, pp. 1–5. arXiv:1901.02967.
URL http://arxiv.org/abs/1901.02967

[18] D. D. Coupland, L. C. Stonehill, N. A. Dallman, W. Feldman, K. Mesick, S. Nowicki, S. Storms, Elpasolite Planetary Ice and Composition Spectrometer (EPICS): a Low-resource combined gamma-ray and neutron spectrometer for planetary science, in: 49th Lunar and Planetary Science Conference, 2018.

[19] S. F. Nowicki, L. C. Stonehill, D. D. Coupland, K. E. Meslck, Development of an Elpasolite Planetary science instrument, 2016 IEEE Nuclear Science Symposium, Medical Imaging Conference and Room-Temperature Semiconductor Detector Workshop, NSS/MIC/RTSD 2016 2017-Janua. doi:10.1109/NSSMIC.2016.8069643.

[20] C. Hardgrove, S. West, L. Heffern, E. Johnson, J. Christian, R. Starr, A. Colaprete, Development of the miniature neutron spectrometer for the lunar polar hydrogen mapper mission, in: Lunar and Planetary Science Conference XLIX, no. 2083, 2018.

[21] C. Hardgrove, J. Bell, R. Starr, A. Colaprete, M. Robinson, D. Drake, I. Lazbin, G. West, E. Johnson, J. Christian, A. Genova, D. Dunham, B. Williams, D. Nelson, A. Babuscia, P. Scowen, K. Cheung, A. Klesh, H. Kerner, A. Deran, R. Amzler, Z. Burnham, J. Lightholder, P. Wren, A. Godber, M. Beasly, The Lunar Polar Hydrogen Mapper (LunaH-Map) CubeSat Mission, in: Lunar and Planetary Science Conference XLVII, 2016, p. 2654.

***Declaration of Interest Statement**

Declaration of interests

☒ The authors declare that they have no known competing financial interests or personal relationships that could have appeared to influence the work reported in this paper.

☐The authors declare the following financial interests/personal relationships which may be considered as potential competing interests: